# Organic-inorganic electronics

by D. B. Mitzi K. Chondroudis C. R. Kagan

Organic-inorganic hybrid materials enable the integration of useful organic and inorganic characteristics within a single molecular-scale composite. Unique electronic and optical properties have been observed, and many others can be envisioned for this promising class of materials. In this paper, we review the crystal structures and physical properties of one family of crystalline, self-assembling, organic-inorganic hybrids based on the layered perovskite framework. In addition to exhibiting a number of potentially useful properties, the hybrids can be deposited as thin films using simple and inexpensive techniques, such as spin coating or singlesource thermal ablation. The relatively new field of "organic-inorganic electronics" offers a variety of exciting technological opportunities. Several recent demonstrations of electronic and optical devices based on organic-inorganic perovskites are presented as examples.

# Introduction

The introduction of different but well-established materials into existing technologies often leads to dramatic improvement in functionality and/or cost. The replacement of aluminum with copper wiring in integrated circuits, for example, while requiring many years of research to overcome materials compatibility issues, has provided a reduction in interconnect delay times and enhanced reliability [1]. The identification of new classes of materials can also profoundly affect existing products as well as enable new disrupting technologies. For example, while progress in phosphor chemistry has provided cathode ray tube (CRT) displays with adequate efficiency,

brightness, and resolution, the depth and weight of CRTs render them inappropriate for portable applications. Ultimately, organic liquid crystals, which share useful properties of crystalline solids and liquids, have provided the basis for most flat panels found in current portable units [2], including laptop and palmtop computers.

Recently, other organic materials have received considerable attention as potential replacements for their inorganic counterparts in flat-panel-display driver circuitry and light-emitting elements. Organic materials have the key advantage of simple and low-temperature thin-film processing through inexpensive techniques such as spin coating, ink-jet printing, or stamping. In addition, the flexibility of organic chemistry enables the formation of organic molecules with useful luminescent and conducting properties. Since the first consideration of organic electroluminescence (EL) devices more than 30 years ago [3], organic light-emitting devices (OLEDs) have been widely pursued, and near-commercial dot-matrix displays have recently been demonstrated [4]. Luminous efficiencies in excess of 30 lm/W and operating voltages as low as 4 V have been reported [5, 6]. In addition to emitting light, the semiconducting properties of some organic materials enable promising technologies for organic field-effect transistors (OFETs). Over the last few years, the carrier mobilities of organic channel layers in OFETs have increased dramatically from 10<sup>-4</sup> to 1 cm<sup>2</sup>/V-s (comparable to those of amorphous silicon) [7, 8].

While very promising with regard to processing, cost, and weight considerations, organic compounds generally have a number of disadvantages, including poor thermal and mechanical stability. In addition, while electrical transport in organic materials has improved, the room-temperature mobility is fundamentally limited by the weak van der Waals interactions between organic molecules (as opposed to the stronger covalent and ionic forces found in

Copyright 2001 by International Business Machines Corporation. Copying in printed form for private use is permitted without payment of royalty provided that (1) each reproduction is done without alteration and (2) the Journal reference and IBM copyright notice are included on the first page. The title and abstract, but no other portions, of this paper may be copied or distributed royalty free without further permission by computer-based and other information-service systems. Permission to republish any other portion of this paper must be obtained from the Editor.

0018-8646/01/\$5.00 © 2001 IBM

30

extended inorganic systems). In OLEDs, the stability and electrical transport characteristics of organic materials contribute to reduced device lifetime. For OFETs, the inherent upper bound on electrical mobility translates to a cap on switching speeds and therefore on the types of applications that might employ the low-cost organic devices. If these issues could be adequately addressed, new technologies might be made possible by organic devices, including lightweight, flexible displays constructed entirely on plastic [9].

Organic-inorganic hybrid materials represent a new class of materials that may combine desirable physical properties characteristic of both organic and inorganic components within a single composite. Inorganic materials offer the potential for a wide range of electronic properties (enabling the design of insulators, semiconductors, and metals), magnetic and dielectric transitions, substantial mechanical hardness, and thermal stability. Organic molecules, on the other hand, can provide high fluorescence efficiency, large polarizability, plastic mechanical properties, ease of processing, and structural diversity. The hybrid materials discussed in this paper encompass organic-inorganic composites that alternate chemically and electronically at the molecular level.

Modulating the electronic structure of materials on the nanometer length scale may evolve unique and potentially superior electronic and optical properties in hybrid materials that are not characteristic of their organic and inorganic building blocks. For example, thermal evaporation of amorphous multilayers of copper pthalocyanine (CuPc) and TiO, with a periodicity of ~50 Å, forms a composite material with a modulated electronic structure analogous to that of type-II quantum well structures [10]. The lowest energy state for holes is the highest occupied molecular orbital (HOMO) of CuPc, while that for electrons is the conduction band of TiO<sub>v</sub>. Photogenerated electron-hole pairs are therefore separated at the organic/inorganic interface. The charge separation induced by the modulated structure, coupled with the higher mobility of the TiO, component, enhances the photoconductive gain of the composite by 40 times compared to that of single-component CuPc layers.

While vacuum techniques may be used to deposit alternating organic and inorganic films, the processes are generally costly, and the chemical/electronic modulation of the composite is limited to one dimension (i.e., normal to the plane of the film). Wet-chemical synthetic routes offer potentially lower-cost and lower-temperature processes for materials preparation. Sol–gel methods, for example, have been used to prepare organic–inorganic silicates for optical applications [11, 12]. The organic component helps mechanically to prevent cracking during thin-film and monolithic solid formation and adds optically interesting

functionality. Selectively (e.g., through masks) bleaching photosensitive organic molecules embedded in a silicate matrix can locally modify the refractive index of the composite and can be used to photopattern waveguiding structures for integrated optics [13, 14]. Nonlinear, optically active (NLO) organic dye molecules may also be oriented within silicate networks by applying an electric field (known as "poling"). Confining the molecules in the inorganic framework improves the nonlinear optical response of the composite, since the inorganic framework restricts the motion of the organic molecules and prevents randomization of molecular orientation due to thermal relaxation [15-18]. The restrictive environment of the silicate network is also useful as a matrix for organic LED and solid-state laser materials. The optically clear silicate framework limits rotations/vibrations that may decrease the photoluminescence quantum yield of dyes. Grafting of both organic chromophores and charge transporters into the silicate structure has been considered for LED applications [19] and can improve the lifetime and stability of the active organic component by preventing segregation and crystallization during device operation. External quantum efficiencies as high as 0.21% have been achieved but with relatively high turn-on voltages of ~18 V.

Wet-chemical techniques are also used to prepare monodisperse organic-inorganic quantum dot (QD) samples of a variety of semiconductor and metallic materials [20, 21]. Organic ligands, used as the solvent and to control the QD growth rate during preparation, coordinate the surfaces of the QDs and may be exchanged for alternate organic molecules with different lengths and electronic structures. The organic ligands also act to sterically stabilize the inorganic QDs in solutions and enable them to be incorporated into polymeric hosts and to be manipulated into two- and three-dimensional organic-inorganic QD superlattices and colloidal crystals [22]. Interactions between neighboring QDs in the solids, whose strengths are mediated by the intervening organic molecules, give rise to novel electronic and optical properties. As the distance between quantum dots is reduced to <100 Å, for example, electronic energy transfer processes shift the emission of semiconducting QD solids [23], and exchange interactions (for distances <5 Å) in metal QD systems give rise to an insulator-metal transition [24]. Semiconductor QDs, such as those containing CdSe and CdS cores with trialkylphosphine chalcogenide capping layers, are good chromophores and have been incorporated as emissive layers in LEDs [25, 26]. The increased photoluminescence quantum yield of CdSe/CdS core/shell QDs enables LEDs with external quantum efficiencies as high as 0.22% and operating voltages of  $\sim 4$  V [27].

While the above examples provide a sampling of the opportunities offered by organic–inorganic hybrids,

they are generally hybrid systems that lack long-range structural ordering, consisting of amorphous organic and/or inorganic components. This paper focuses on a particularly promising class of *crystalline* organic–inorganic hybrids—the organic–inorganic perovskites [28]. Crystalline materials have the advantage that they can be structurally characterized using techniques such as X-ray or neutron diffraction, making it possible to correlate structural features with specific materials properties. In addition, the crystalline nature and the rigid, extended inorganic framework provide an opportunity for higher electrical mobility, better thermal stability, and templating of the organic component of the structure.

# Organic-inorganic perovskites: Structures and properties

The basic layered perovskite structures [28], (R-NH<sub>3</sub>)<sub>2</sub>MX<sub>4</sub> and  $(NH_2-R-NH_2)MX_4$   $(X = Cl^-, Br^-, or I^-)$ , are schematically depicted in Figure 1. Each of the inorganic layers consists of sheets of corner-sharing metal halide octahedra. In order to satisfy charge-balancing requirements, the M cation is generally a divalent metal that can adopt an octahedral anion coordination, such as Cu<sup>2+</sup>, Ni<sup>2+</sup>, Co<sup>2+</sup>, Fe<sup>2+</sup>, Mn<sup>2+</sup>, Cr<sup>2+</sup>, Pd<sup>2+</sup>, Cd<sup>2+</sup>, Ge<sup>2+</sup>, Sn<sup>2+</sup>, Pb<sup>2+</sup>, Eu<sup>2+</sup>, or Yb<sup>2+</sup>. Recently this family has been extended to include the trivalent metals, Bi<sup>3+</sup> and Sb<sup>3+</sup> [29], wherein the charge difference is accommodated by vacancies on the metal site. These inorganic layers are often referred to as "perovskite sheets" because they are conceptually derived from the three-dimensional AMX, perovskite structure by taking a one-layer-thick cut along the  $\langle 100 \rangle$  direction of the three-dimensional crystal lattice. In addition to single-layer perovskite sheets, the structures can also be conveniently synthesized with multiple (100)oriented sheets [Figure (2a)] [30–32], enabling control over the dimensionality of the inorganic framework, or with differently oriented cuts (e.g., (110) vs. (100)) of the three-dimensional perovskite structure [Figure (2b)] [33, 34]. These structural modifications are simply achieved by altering the combination of organic and inorganic salts in the starting solution from which the hybrids are crystallized. The large repertoire of inorganic frameworks enables tailoring of the electronic, optical, and magnetic properties.

The organic component of the  $\langle 100 \rangle$ -oriented structures may consist of a bilayer (for monoammonium) or monolayer (for diammonium) of organic cations (see Figure 1). In the case of monoammonium cations, R-NH $_3^+$  [Figure (1a)], the ammonium head of the cation hydrogen/ionically bonds to the halogens in one inorganic layer, and the organic R-group extends into the space between the inorganic layers. For diammonium cations,  $^+$ NH $_3$ -R-NH $_3^+$  [Figure (1b)], the molecules span the

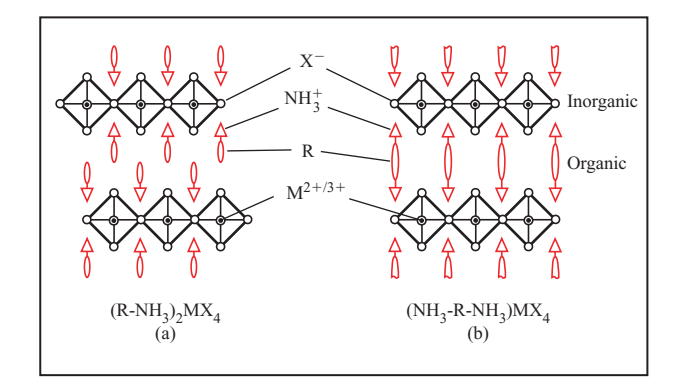


## Figure '

Schematic representation of single-layer (n=1) <100>-oriented perovskites with (a) monoammonium (R-NH $_3$ ) or (b) diammonium ( $^+$ NH $_3$ -R-NH $_3$ ) organic cations. Note that divalent ( $^{2+}$ ) metals generally occupy the metal site. For certain systems, however, a mixture of trivalent ( $^{3+}$ ) cations and vacancies can occupy the metal site, yielding  $M_{2/3}X_4^{2-}$  layers.

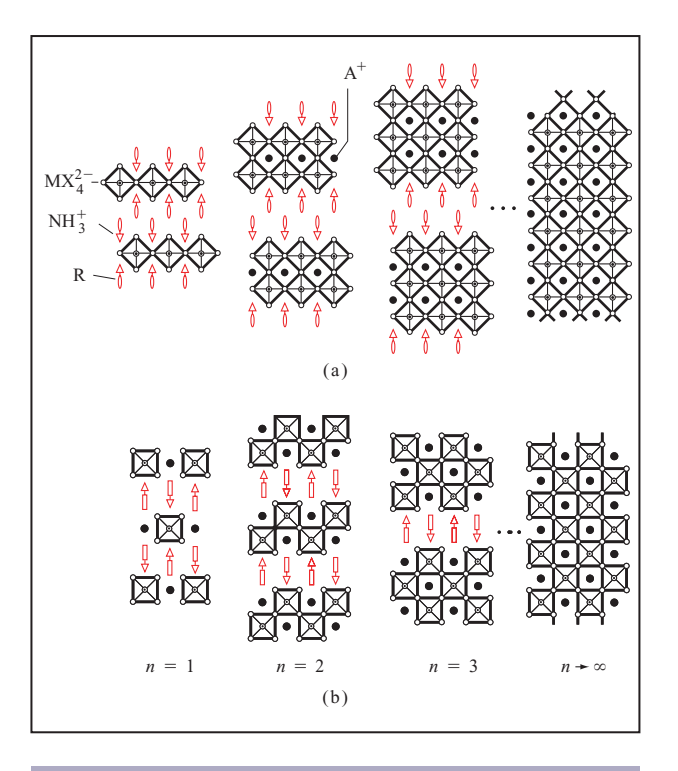
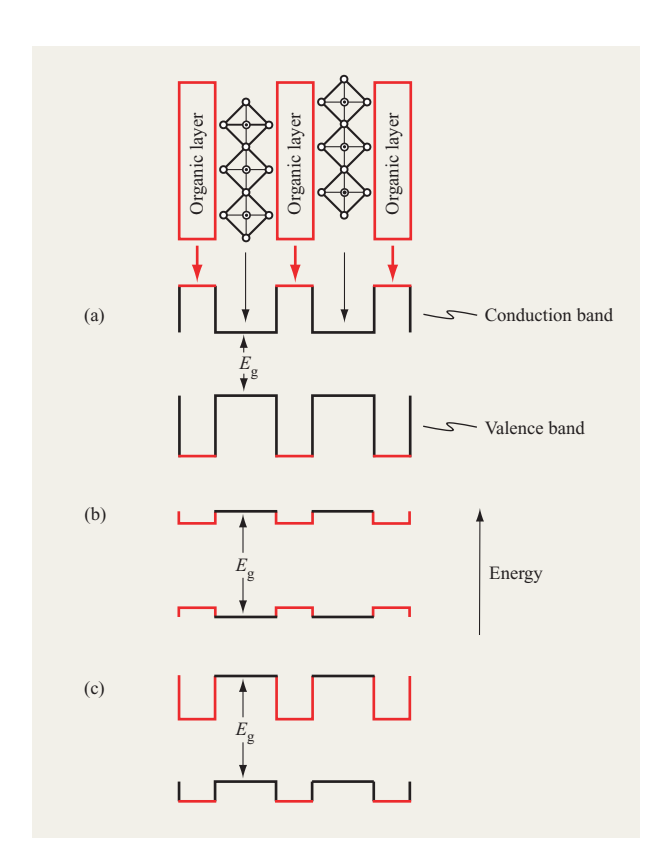


#### Figure 2

Schematic representation of (a) <100>- and (b) <110>-oriented families of layered organic—inorganic perovskites. For the <100>-oriented [(R-NH<sub>3</sub>)<sub>2</sub>A<sub>n-1</sub>M<sub>n</sub>X<sub>3n+1</sub>] and <110>-oriented [(R-NH<sub>3</sub>)<sub>2</sub>A<sub>n</sub>M<sub>n</sub>X<sub>3n+2</sub>] structures, R is an organic group, A<sup>+</sup> is a small organic (e.g., CH<sub>3</sub>NH<sub>3</sub>) or inorganic (e.g., Cs<sup>+</sup>) cation, M is generally a divalent metal cation, X is a halide (Cl<sup>-</sup>, Br<sup>-</sup>, I<sup>-</sup>), and n defines the thickness of the perovskite sheets. The R-group can be used to control which of the two structural families forms [33]. Note that the  $n \rightarrow \infty$  compound, AMX<sub>3</sub>, is the same for each family.





Schematic organic—inorganic perovskite structure and several possible energy-level schemes that can arise within these structures. The most common arrangement is shown in (a), where semiconducting inorganic sheets alternate with organic layers having much wider bandgaps, resulting in a type I quantum well structure. In (b), widerbandgap inorganic layers and organic cations with a smaller HOMO–LUMO gap result in the well/barrier roles of the organic and inorganic layers being switched. In (c), by shifting the electron affinity of the organic layers relative to the inorganic layers, a staggering of the energy levels leads to a type II quantum well structure.

distance between adjacent inorganic layers; therefore, no van der Waals gap exists between the layers. The organic R-group most commonly consists of an alkyl chain or a single-ring aromatic group. These simple organic layers help to define the degree of interaction between and the properties arising in the inorganic layers.

The unique structural and chemical characteristics of the organic-inorganic perovskites provide for equally interesting and potentially useful physical properties. Many of the layered hybrid perovskites, especially those containing germanium(II), tin(II), or lead(II) halide sheets, are analogous to multilayer quantum well structures, with semiconducting, or even metallic, inorganic sheets alternating with organic layers having a relatively large HOMO-LUMO (lowest unoccupied molecular orbital) energy gap [Figure (3a)]. These self-

assembling structures share many of the interesting properties of quantum well structures prepared by "artificial" techniques, such as molecular beam epitaxy (MBE), but without the tendency for interfacial roughness between the well and barrier layers. In fact, the organic–inorganic perovskites can be conveniently grown in single-crystalline form.

Note that in Figure (3a) the conduction band of the inorganic layers is substantially below that of the organic layers, and the valence band of the inorganic layers is similarly above that of the organic layers. Therefore, the inorganic sheets act as quantum wells for both electrons and holes. In principle, other arrangements of organic and inorganic energy levels are possible. If metal halide sheets having a larger bandgap are integrated with more complex, conjugated (i.e., smaller HOMO-LUMO energy gap) organic cations, the well and barrier layers can be reversed [Figure (3b)]. Alternatively, given appropriate constituents, the bandgaps for the organic and inorganic layers can be offset [Figure (3c)], leading to a type II heterostructure in which the wells for the electrons and holes are in different layers. Finally, as a further example of flexibility, the width of the barrier and well layers can easily be adjusted by changing the length of the organic cations and the number of perovskite sheets between each organic layer. These important modifications can be implemented by simply changing the composition or stoichiometry of the organic and inorganic salts in the solution used to grow the hybrid crystals or films.

The perovskite quantum well structures, with optically inert (i.e., large HOMO-LUMO energy gap) organic cations and semiconducting inorganic sheets, exhibit sharp resonances (Figure 4) in their room-temperature optical absorption spectra, which arise from an exciton state associated with the inorganic semiconducting layers. Since these excitons are associated with the bandgap of the inorganic framework, the spectral positions of the transitions can be tailored by substituting different metal cations or halides within the inorganic framework [35, 36]. The strong binding energy of the excitons, which enables the optical features to be observed at room temperature, arises because of the two-dimensionality of the inorganic structure, coupled with the dielectric modulation between the organic and inorganic layers [37]. In addition to the sharp transition in the absorption spectra, the large exciton binding energy and oscillator strength lead to strong photoluminescence, nonlinear optical effects [32], and tunable polariton absorption [38].

The electrical transport properties of the layered perovskites have also been examined, with an unusual semiconductor-metal transition (**Figure 5**) being noted in the families,  $(R-NH_3)_2(CH_3NH_3)_{n-1}Sn_nI_{3n+1}$  and  $[NH_2C(I)=NH_2]_2(CH_3NH_3)_nSn_nI_{3n+2}$ , as a function of increasing perovskite layer thickness (i.e., increasing n—

see Figure 2) [31, 33]. While most metal halides are good insulators, the tin(II) halide-based perovskites exhibit high carrier mobilities and, in some cases, even metallic conduction. The three-dimensional perovskite,  $\text{CH}_3\text{NH}_3\text{SnI}_3$ , for example (i.e., the  $n \to \infty$  member of the previously mentioned families), is a low-carrier-density p-type metal with a Hall hole density of  $1/R_h e \approx 2 \times 10^{19} \text{ cm}^{-3}$  and a Hall mobility of  $\mu \approx 50 \text{ cm}^2/\text{V-s}$  at room temperature [39]. It should be noted that the mobility value quoted above has been measured using a pressed pellet sample and can therefore be considered a lower bound on the mobility in these semiconducting/metallic hybrid perovskite structures.

While most of the perovskites studied to date contain relatively simple (large HOMO-LUMO gap) organic cations, such as alkylammonium or phenethylammonium cations, in principle, more complex organic molecules can be incorporated, subject to certain chemical and structural constraints. First, the organic molecule must contain one or two terminal cationic groups that can ionically interact with the extended inorganic anion. Additionally, these groups should be able to effectively hydrogen-bond to the inorganic framework. For most known layered perovskite structures, the tethering group is a protonated primary amine. Second, the organic molecule must fit within the "footprint" provided by the inorganic framework, with the lateral dimensions of the molecule being limited by the potential for steric interactions between nearest-neighbor molecules. In contrast, the length of the molecule (which should extend away from the perovskite sheets) can take on a wide range of values, since the distance between perovskite sheets can vary. Therefore, long and narrow molecules are expected to be favored over molecules with a large cross-sectional area. Finally, interactions between the organic R-groups can either stabilize or destabilize the perovskite structure. These interactions can include hydrogen bonding, aromatic-aromatic, or van der Waals interactions.

Recently, the oligothiophene derivative, 5,5"'-bis(aminoethyl)-2,2':5',2":5",2"'-quaterthiophene (AEQT), shown in **Figure** (**6a**), has been incorporated within a layered perovskite framework [**Figure** (**6b**)] consisting of  $MX_4^{2-}$  (M = Cd, Pb, Sn; X = Cl, Br, I) or  $M_{2/3}X_4^{2-}$  ( $M = Bi^{3+}$ , Sb<sup>3+</sup>) sheets [28, 29, 40]. The diprotonated AEQT cation has an appropriate tethering group (ethylammonium) and long, narrow profile ideally suited for incorporation within the layered perovskite framework. Each quaterthiophene oligomer is ordered between the metal halide sheets in a herringbone arrangement with respect to neighboring quaterthiophenes [40]. This ordered arrangement is at least partially templated by the relatively rigid inorganic framework.

Annealed thin films of the  $(H_2AEQT)PbX_4$  (X = Cl, Br, I) materials exhibit the characteristic exciton absorption

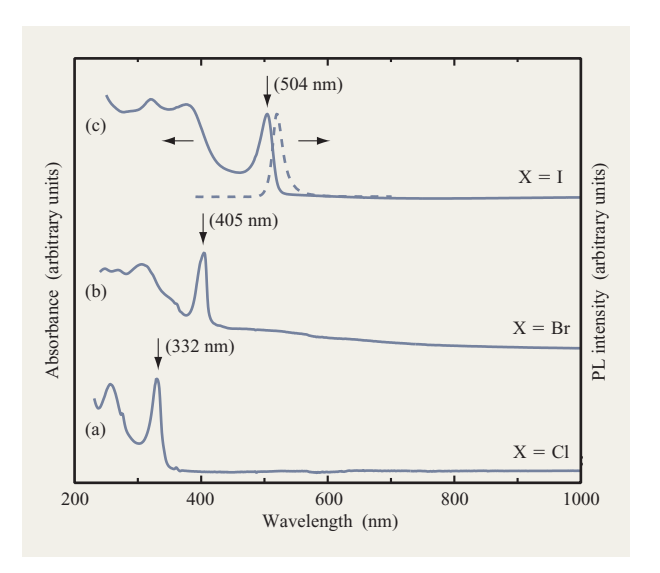


#### Figure 4

Room-temperature UV-vis absorption spectra for thin films of  $(C_4H_9NH_3)_2PbX_4$  with (a) X=Cl, (b) X=Br, (c) X=I. In each spectrum, the arrow indicates the position of the exciton absorption peak (with the wavelength in parentheses). In (c), the corresponding photoluminescence (PL) spectrum ( $\lambda_{ex}=370$  nm) is indicated by the dashed curve. Note the small (~15 nm) Stokes shift between the absorption and emission peaks for the excitonic transition.

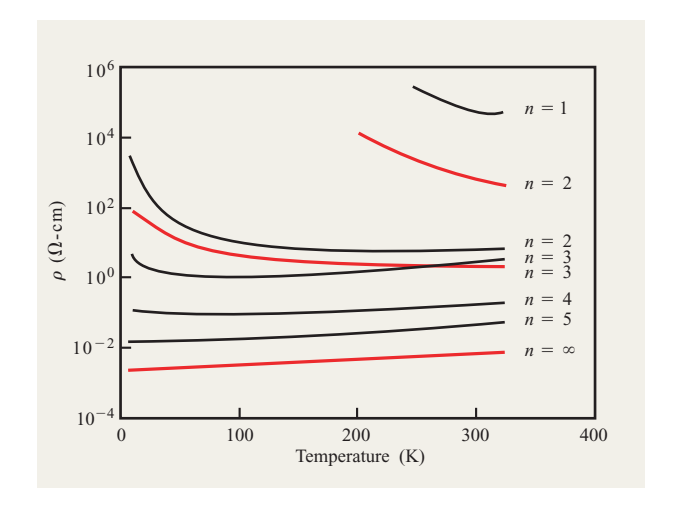
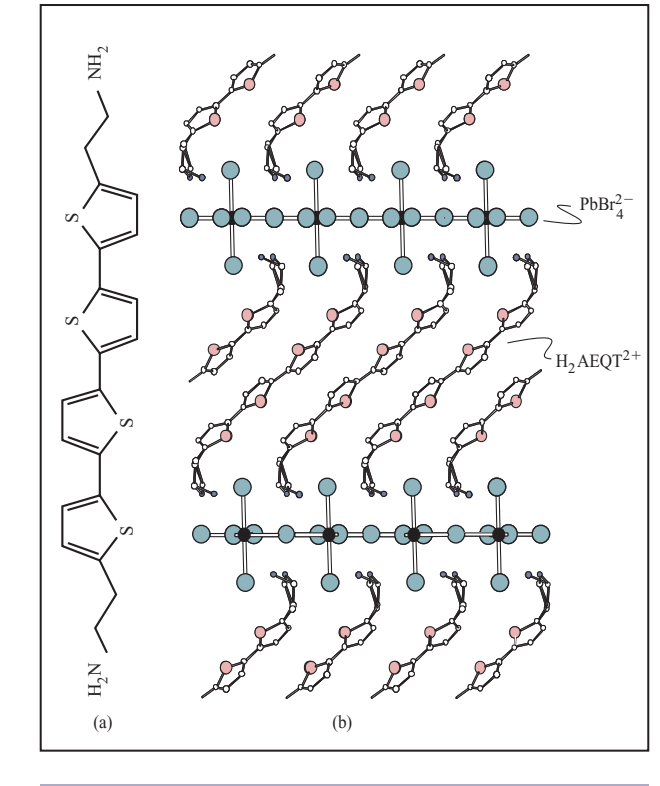


#### Figure 5

Resistivity ( $\rho$ ) as a function of temperature for pressed pellet samples of the layered perovskite families  $(C_4H_9NH_3)_2(CH_3NH_3)_{n-1}Sn_nI_{3n+1}$  (black curves) and  $[NH_2C(I)=NH_2]_2(CH_3NH_3)_nSn_nI_{3n+2}$  (red curves), as well as for the  $n \rightarrow \infty$  end-member of both families  $(CH_3NH_3SnI_3)$ . (Adapted with permission from [33]. © 1995 American Association for the Advancement of Science.)

resonance associated with the inorganic perovskite sheets, along with absorption from the chromophore molecule [40]. In contrast, the photoluminescence spectrum exhibits



(a) The 5,5"'-bis(aminoethyl)-2,2':5',2":5",2"'-quaterthiophene molecule (AEQT). (b) Perovskite structure of  $(H_2AEQT)PbBr_4$  [i.e.,  $(C_{20}H_{22}S_4N_2)PbBr_4$ ], with the doubly protonated AEQT cation occupying the organic cation site of the structure.

no emission from the inorganic exciton state for any of the quaterthiophene-containing perovskites. Rather, for X=Cl, strong photoluminescence is observed only from the quaterthiophene moiety. The AEQT luminescence is progressively quenched across the  $X=Cl \rightarrow Br \rightarrow I$  series, as the bandgap of the inorganic framework decreases in energy compared to the HOMO-LUMO gap of the chromophore molecule (e.g., see Figure 3). This quenching is associated with energy transfer and/or charge separation [40] between the organic and inorganic components of the structure.

Other chromophore-containing perovskites have also recently been considered [41, 42], including the compounds  $(R-NH_3)_2PbCl_4$  (R=2-phenylethyl, 2-naphthylmethyl, and 2-anthrylmethyl) [42]. This is a particularly interesting series because, for <math>R=2-phenylethyl, the singlet and triplet states of the organic cation are higher in energy than the exciton state of the inorganic sheets; therefore, emission from the inorganic exciton is observed in the photoluminescence spectrum. For R=2-naphthylmethyl, the inorganic exciton state apparently falls between the organic

singlet and triplet states, and phosphorescence from the organic molecules dominates the emission spectrum. Finally, for R=2-anthrylmethyl, the inorganic exciton state is higher in energy than both the organic singlet and triplet states, and chromophore singlet emission is dominant.

An interesting feature of the oligomer- or dyecontaining organic-inorganic perovskites is the fact that the orientation of the organic cation can be controlled or templated as a result of the inorganic framework. This can have a substantial impact on physical properties or potential applications of these materials. For example, if organic chromophores can be held in an orientation that minimizes electronic interaction with neighboring chromophores, concentration quenching of the fluorescence efficiency may be reduced. Furthermore,

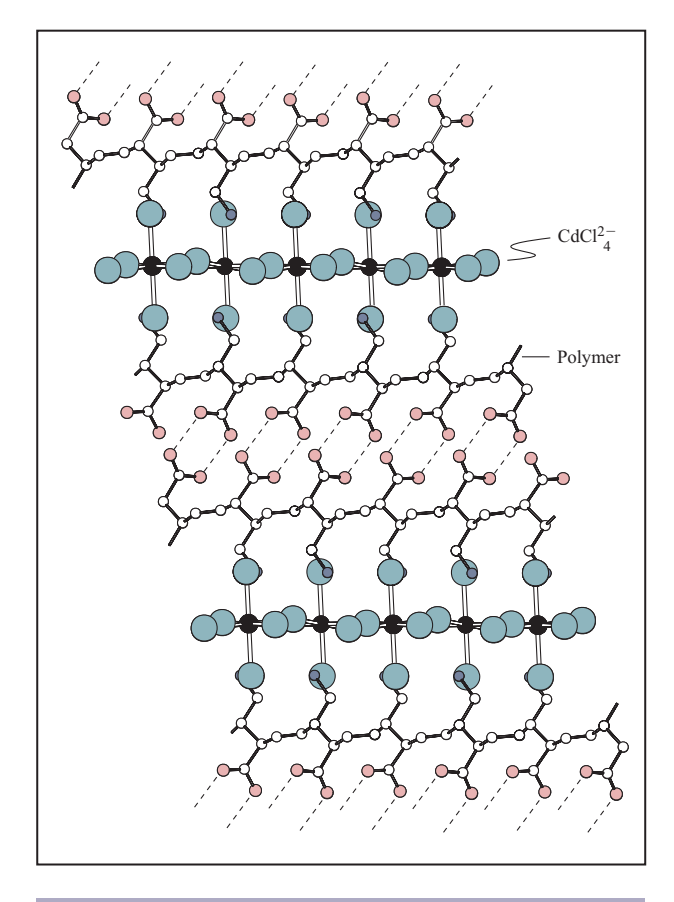


## Figure 7

Crystal structure of the ordered polymerized product formed by subjecting (HOOC-CH=CH-CH=CH-CH<sub>2</sub>NH<sub>3</sub>)<sub>2</sub>CdCl<sub>4</sub> to UV or  $\gamma$  irradiation [45]. Polymerization yields the 1,4-disubstituted *trans*-polybutadiene [-CH(COOH)-CH=CH-CH(CH<sub>2</sub>NH<sub>2</sub>)-]<sub>∞</sub>. Hydrogen bonding between COOH groups on adjacent layers is shown by dashed lines. For clarity, hydrogen atoms have been left out of the figure. (Adapted from [28]. © 1999 John Wiley & Sons, Inc. This material is used by permission of John Wiley & Sons, Inc.)

in hybrids containing organic molecules with an extended  $\pi$  system, templating may be used to affect the electrical transport properties of the organic layer. In OFET devices, the mobility of the organic channel layer is strongly affected by the degree of molecular ordering of the oligomer layer. In vacuum-deposited organic films, some control over oligomer ordering has been attained by varying the substrate temperature during sublimation [43] or through the appropriate attachment of functional groups to the oligomer [44]. The organic–inorganic perovskite systems described above demonstrate that the inorganic sheets can be used to template the formation of single-crystalline layers of organic molecules, potentially providing a pathway to higher mobilities within oligomer layers.

Another interesting example of the templating influence of the inorganic sheets involves solid-state polymerization within the organic layer of perovskite structures [45, 46]. In this case, rather than employing saturated organic R-groups in the (R-NH<sub>3</sub>)<sub>2</sub>MX<sub>4</sub> structures, more reactive groups (such as diene or divne groups) are employed. In one example, the hydrochloride salt of 6-amino-2,4-trans, trans-hexadienoic acid, within a cadmium(II) chloride perovskite framework, polymerizes under ultraviolet (UV) or  $\gamma$  irradiation. The polymerization occurs through a 1,4 addition mechanism, leading to a well-ordered polymer layer (Figure 7) [45]. The same photoreactive organic cation in a copper chloride framework does not undergo polymerization. The structural differences in the inorganic framework, induced by the Jahn-Teller distortion of the copper(II) chloride octahedra, lead to an unfavorable (with respect to the polymerization process) configuration of the monomer within the organic layer. Consequently, the inorganic framework can be used to control whether or not a monomer-containing hybrid system is susceptible to polymerization.

# Thin-film deposition

The relevant interactions giving rise to crystalline assembly within the hybrid perovskites include covalent/ionic bonding (which favors the formation of sheets of corner-sharing metal halide octahedra), hydrogen/ionic bonding between the organic cations and the halogens in the inorganic sheets, and various weaker interactions (van der Waals,  $\pi$ – $\pi$ , etc.) between the organic R-groups. Given the good solubility of many metal halides in polar organic and aqueous solvents, as well as the strong tendency to self-assemble, single crystals of the organicinorganic perovskites can generally be grown from near-ambient-temperature saturated solutions containing the relevant metal halide and organic salts [28, 47]. While single crystals are generally the most useful medium for examining structural and physical properties of the hybrids, many electronic and optical applications require

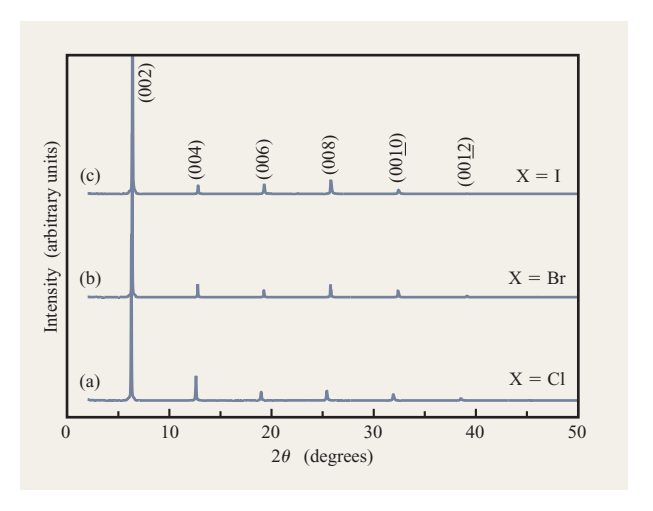


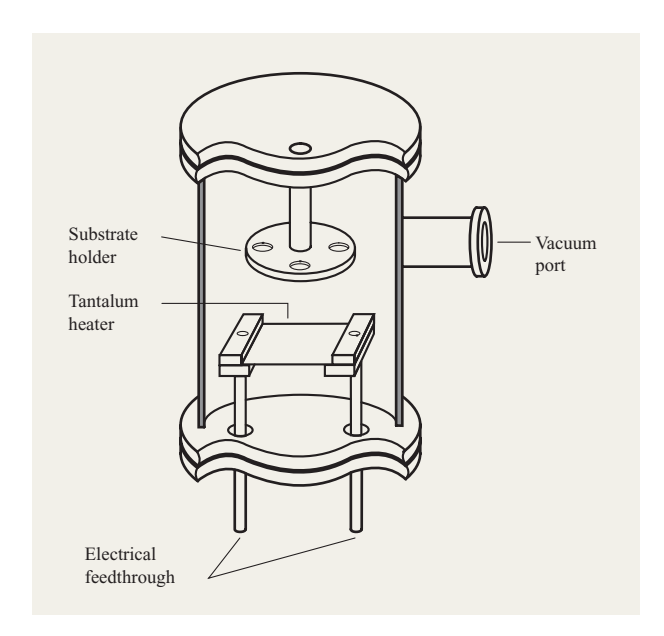
#### Figure 8

Powder X-ray patterns for spin-coated thin films of  $(C_4H_9NH_3)_2PbX_4$ , where (a) X = Cl, (b) X = Br, and (c) X = I. The X-ray reflection indices are given above the data for X = I, and are the same for each sample. The X-ray patterns depicted here correspond to the samples used to generate the optical data presented in Figure 4. (Reproduced from [28]. © 1999 John Wiley & Sons, Inc. This material is used by permission of John Wiley & Sons, Inc.)

the ability to deposit thin films. One of the important advantages of organic–inorganic perovskites and related hybrid materials is the possibility of processing the materials using a number of simple solution-based or evaporative thin-film techniques [28].

Spin-coating enables film deposition of hybrid perovskites on various substrates, including glass, quartz, plastic, sapphire, and silicon. The relevant parameters for this technique include the choice of substrate, the solvent, the concentration of the hybrid in the solvent, the substrate temperature, and the spin speed. In some cases, pretreating the substrate surface with an appropriate adhesion promoter improves the wetting properties of the solution on the desired substrate. In addition, postdeposition low-temperature annealing ( $T < 250^{\circ}$ C) of the hybrid films is sometimes employed to improve crystallinity and phase purity. As an example, Figure 8 shows the X-ray diffraction patterns for unannealed films of  $(C_4H_0NH_2)_2PbX_4$  (X = Cl, Br, I), spin-coated from acetone (X = I) or N,N-dimethylformamide (X = CI)or Br) solutions onto untreated quartz substrates. The spin-coated films are generally smooth (~1-2 nm RMS roughness) and suitable for optical studies or device fabrication. In addition to spin-coating, other possible solution-based deposition techniques for the organic-inorganic perovskites include ink-jet printing, stamping, and spray coating. All of these techniques require a suitable solvent for the organic-inorganic hybrid.





Cross-sectional view of a typical single-source thermal ablation (SSTA) chamber. (Reproduced with permission from [49]. © 1999 American Chemical Society.)

In some cases, a solvent cannot be identified for a solution-based deposition technique. This may result either from a lack of solubility of the hybrid or from problems with substrate wetting. Furthermore, for some applications or studies, vacuum-compatible thin-film techniques may be appropriate. The problem with evaporative film deposition for the hybrid materials is that the organic component of the structure generally dissociates or decomposes from the material at substantially lower temperatures or in a shorter time period relative to the inorganic component of the structure. Two approaches have been employed to overcome this thermal or temporal incompatibility between the two components during evaporation. In twosource thermal evaporation, the organic ammonium salt and the metal halide components of the hybrid are contained in separate evaporation sources, and each is heated to an appropriate temperature to enable a nominally controlled evolution. Multiple substrates can be placed above the two sources within the vacuum system. Assuming that the evaporation rate for the two components can be controlled and calibrated, a stoichiometric and often crystalline film of the organic-inorganic composite can be prepared [48].

While the metal halide salt generally evaporates in a well-defined fashion, the organic salt deposition is often difficult to control, potentially resulting in poor film homogeneity and irreproducible film characteristics. In addition, each distinct organic—inorganic hybrid system

requires new heater parameters to balance the evolution rates of the two components. Recently, a single-source thermal ablation (SSTA) technique has been described [49] that employs a single evaporation source and very rapid heating. A deposit of the organic-inorganic hybrid is placed on a thin tantalum heater within a vacuum chamber (Figure 9). When a large current is passed through the heater, the hybrid ablates from the source over a very short interval (<1 s) and deposits on the substrates positioned above the heater. Since the ablation process is essentially instantaneous, both the organic and inorganic components evaporate from the heater simultaneously and, in general, without significant decomposition of the organic component. Surprisingly, in many cases (especially with relatively simple organic cations), the as-deposited films are single-phase and crystalline (Figure 10), indicating that the organicinorganic hybrids can reassemble on the substrate even at room temperature [49]. For more complex organic cations, a short (<20 min), low-temperature (<200°C) anneal is sometimes required to improve the film crystallinity [50].

Some organic components will not withstand the heating required for evaporative or sublimation processes. As an alternative, a dip-processing technique [51] has been demonstrated in which metal halide films, predeposited on a substrate, are dipped into an ambient-temperature solution containing the organic cation. The solvent for the dipping solution is chosen so that the organic salt is substantially soluble, but the starting metal halide and the final organic-inorganic hybrid are not. The organic cations react with the metal halide on the substrate and form a single-phase crystalline film of the desired hybrid. For the family  $(R-NH_3)_2(CH_3NH_3)_{n-1}M_nI_{3n+1}$  (R = butyl,phenethyl; M = Pb, Sn; n = 1, 2), toluene/2-propanol mixtures work well as the solvent, and the dipping times are relatively short (several seconds to several minutes, depending on the system and film thickness) [51]. The advantages of the dip-processing technique include that a simultaneously suitable solvent for both the organic and inorganic components of the hybrid is not required and that the organic cations need not be heated.

## Organic-inorganic devices

The desirable electrical and optical properties exhibited by the hybrid perovskites, along with the potential for simple, low-cost processing techniques, make it interesting to consider building devices with these materials. One possibility involves the use of organic–inorganic hybrids in LEDs. As previously mentioned, excitonic transitions, associated with the inorganic sheets of the  $(R-NH_3)_2MX_4$  (M=Ge,Sn,Pb;X=Cl,Br,I) perovskites, give rise to strong photoluminescence that can be tuned by incorporating different metal or halogen atoms in the

structure. These useful optical characteristics make the perovskites attractive as potential emissive materials in electroluminescent (EL) devices. The first attempts to induce EL in these materials involved attaching silver paint contacts to single crystals of  $(C_{\epsilon}H_{\epsilon}C_{\gamma}H_{\delta}NH_{\gamma})_{\gamma}(CH_{\gamma}NH_{\gamma})Pb_{\gamma}I_{\gamma}$  [52]. By applying an electric field (>10 kV-cm<sup>-1</sup>) in the plane of the perovskite sheets and cooling the sample to below 200 K, orange emission was observed, apparently as a result of an avalanche breakdown mechanism. More recently, EL devices were prepared, with a structure analogous to that of traditional OLEDs, but with hybrid (R-NH<sub>3</sub>)<sub>2</sub>PbI<sub>4</sub> perovskite light-emitting layers [53, 54]. In these examples, the perovskite organic bilayer consisted of optically inert (in the visible spectrum) phenethylammonium  $(C_6H_5C_2H_4NH_3^+)$  or cyclohexenylethylammonium (C<sub>4</sub>H<sub>0</sub>C<sub>2</sub>H<sub>4</sub>NH<sub>2</sub><sup>+</sup>) cations. The heterostructure device consisted of an indium tin oxide (ITO) anode, a spin-coated (R-NH<sub>3</sub>)<sub>2</sub>PbI<sub>4</sub> emissive layer, an evaporated 1,3,4-oxadiazole,2,2'-(1,3-phenylene)bis[5-[4-(1,1-dimethylethyl)phenyl]] (OXD7) electron transport layer, and a MgAg cathode. When the OILED (Organic-Inorganic Light-Emitting Diode) was driven at liquid nitrogen temperature, it exhibited intense and efficient EL at an applied voltage of 24 V. Unfortunately, the emission intensity dropped off rapidly with increasing temperature, rendering such devices impractical for display applications. The dramatic reduction in EL efficiency near room temperature results, most probably, from thermal quenching of the excitons (i.e., the temperature dependence is very similar to that for the photoluminescence quantum yield).

In these initial devices, light emission arises from excitons within the inorganic component of the structure. To obtain room-temperature EL from the hybrids, we designed and synthesized the dye molecule AEQT (Figure 6), based on an oligothiophene moiety, to replace the optically inert alkyl or simple aromatic component typically used in layered perovskite structures [28, 40]. The goal of this substitution was to incorporate additional functionality (fluorescence efficiency) within the organic layer of the perovskite, thereby increasing the likelihood of efficient room-temperature emission. Films of (H<sub>2</sub>AEQT)PbCl<sub>4</sub> were deposited using the single-source thermal ablation (SSTA) method, followed by a short (5 min), low-temperature (115°C), inert-atmosphere anneal, using a digitally controlled hot plate. The UV-vis absorption spectra of the annealed SSTA-deposited films exhibited the characteristic exciton absorption (331 nm) for the lead-chloride-based perovskite framework (Figure 11), demonstrating that the correct structure had formed. However, the films had a featureless X-ray powder diffraction pattern, indicating a small grain size or short-

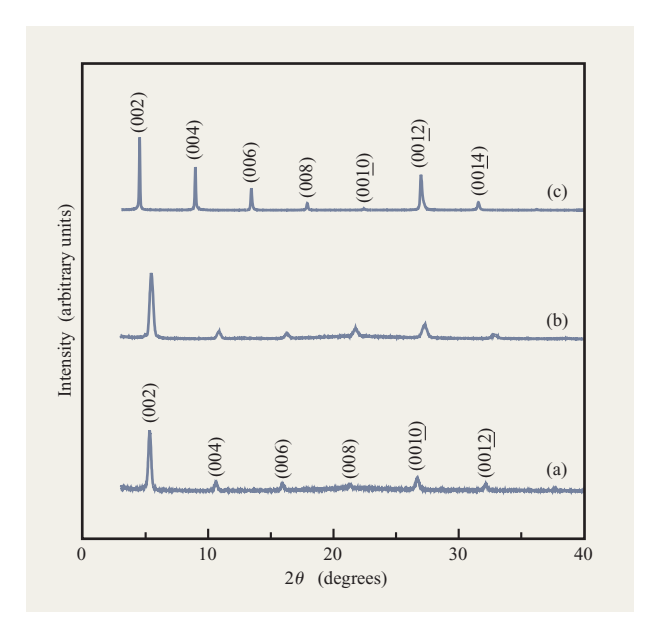
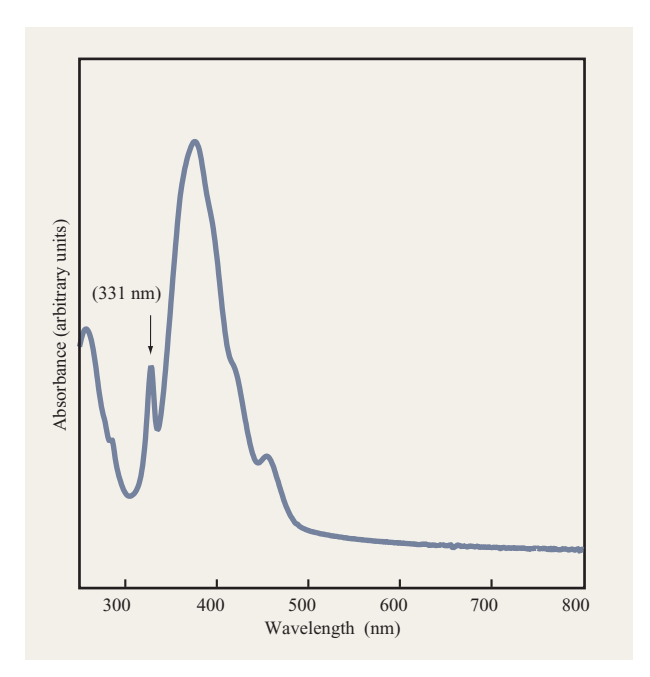


# Figure 10

X-ray diffraction patterns for hybrid perovskite thin films deposited using the SSTA technique: (a)  $(C_6H_5C_2H_4NH_3)_2PbBr_4$ ; (b)  $(C_6H_5C_2H_4NH_3)_2PbI_4$ ; (c)  $(C_4H_9NH_3)_2(CH_3NH_3)Sn_2I_7$ . The X-ray reflection indices for pattern (b) are the same as those for pattern (a). All of the films were measured "as-deposited" (i.e., with no postdeposition annealing).

range ordering of the perovskite structure. The smooth film morphology and fine-grain structure were also confirmed with atomic force microscope (AFM) and scanning electron microscope (SEM) studies. Higher annealing temperatures resulted in a gradual increase of the grain size, as observed previously for a related thiophene-containing perovskite system [50].

The device structure employed [55] can be seen in Figure 12. It consists of a circular (3/4-in.-diameter), optically polished quartz substrate on which ITO has been e-beam-deposited (1500 Å, 14  $\Omega/\Box$ ) as an anode. To avoid shorting between the anode and cathode, 1300 Å of SiO, was e-beam-deposited on top of the ITO through contact masks, thereby defining four rectangular areas (3 mm  $\times$  1 mm) of exposed ITO. After cleaning the substrates using solvent-based and oxygen plasma processes, a patterned 3000-Å (H<sub>2</sub>AEQT)PbCl<sub>4</sub> film was deposited on the exposed ITO areas using SSTA at  $10^{-7}$  Torr, followed by the short low-temperature annealing cycle. Subsequently, 200 Å of OXD7 was vacuum-deposited by resistive heating at 10<sup>-7</sup> Torr. To complete the devices, an Mg:Ag [20:1] alloy was coevaporated (600 Å,  $10^{-7}$  Torr) through a contact mask with four rectangular 2-mm × 7-mm openings. These openings were at a 90° angle to the exposed ITO, thus providing an active device area of



Room-temperature UV-vis absorption spectrum for an annealed SSTA-deposited film of  $(H_2AEQT)PbCl_4$  on a quartz substrate. The peak from the inorganic sheet exciton is marked with an arrow. The broader features at wavelengths above 350 nm correspond to the AEQT absorption.

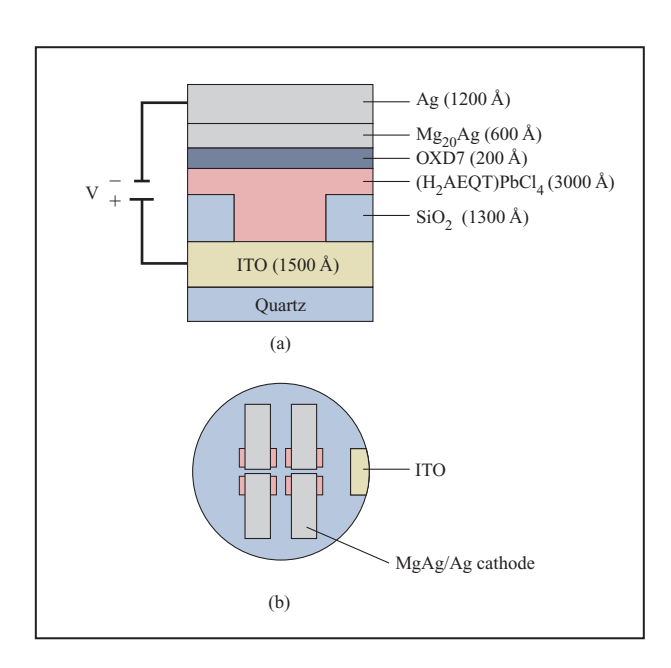


#### Figure 12

(a) Cross section of the OILED device structure (not to scale); (b) top view of the circular substrate containing four devices. For clarity, the OXD7 layer (on top of the patterned hybrid perovskite layer) is not shown.



# Figure 13

Photograph of an operational OILED device based on  $(H_2AEQT)PbCl_4$  as the emitting material. The nickel on the right provides a scale for size comparison.

 $1~\mathrm{mm} \times 2~\mathrm{mm}$  [Figure 12(b)]. Another 1200 Å of Ag was deposited on top to inhibit oxidation. It should be noted that the vacuum system employed for device construction was connected to the antechamber of a nitrogen-filled glovebox, allowing for preparation of the devices under completely inert conditions. The devices were crudely encapsulated using a cover glass and epoxy before evaluation.

Bright green-yellow light ( $\lambda_{max} \approx 530 \text{ nm}$ ) was observed in a well-lit room when the devices were forward-biased under ambient conditions (Figure 13). Figure 14 shows the electroluminescence-voltage characteristics for the OILED structure. A low turn-on voltage of about 5.5 V was observed. The I-V and EL-V curves are essentially superimposable, indicating a relatively balanced electron and hole injection [55]. The electroluminescence spectrum corresponds well to the photoluminescence spectrum of (H<sub>2</sub>AEQT)PbCl<sub>4</sub> [Figure 14(b)], as well as to that of the dye salt AEQT-2HCl, indicating that the EL arises from the quaterthiophene moiety. The maximum efficiency was 0.1 lm/W at 8 V and 0.24 mA (power conversion efficiency 0.11%). Devices with a 600-Å (H<sub>2</sub>AEQT)PbCl<sub>4</sub> film had a lower turn-on voltage of 4.8 V compared to the devices with a 3000-Å emission layer. Interestingly, even with the thicker film, the turn-on voltage remained relatively low. The fact that thicker organic-inorganic emission layers can be used than in conventional OLEDs (typically <600 Å) should improve device reliability and lifetime, since it renders the devices less prone to pinholes and shorts.

The molecular-level sequencing of organic and inorganic layers may be advantageous for several reasons. First, the artificial layering (i.e., by successive evaporation) of organic dye molecules (e.g., Alq<sub>3</sub>) and wide-bandgap inorganic compounds (e.g., LiF) has recently been shown

[56] to enhance EL efficiency and device lifetime compared to systems with a single layer of the emitting dye. The improved device performance can apparently be attributed to better carrier injection, transport, and electron-hole recombination. The self-assembling hybrid perovskites provide a much simpler way (a single evaporation step) of achieving this type of alternating structure. Interestingly, hybrid perovskite devices designed with lead bromide (narrower bandgap) inorganic sheets exhibited efficiencies 20 to 30 times lower than the ones with lead chloride sheets, whereas preliminary results for analogous devices with cadmium chloride (wider bandgap) layers produced higher efficiencies of  $\sim 0.16$  lm/W. This further suggests that, as for the OILEDs made with alternating Alq<sub>3</sub>/LiF layers, the self-assembling organic-inorganic structures can have a large impact on the luminous efficiencies exhibited by the emitting species within the structure. The choice of inorganic framework also has a substantial effect on the electronic properties of the perovskite and hence on the electrical characteristics of the device. As can be seen in Figure 14(a), the higher bandgap of cadmium chloride gives rise to a higher turnon voltage of about 9 V (compared to 5.5 V) for the device containing this framework, despite the use of a thinner emissive layer (1200 Å versus 3000 Å).

A further feature of the hybrid perovskites is that since the dye molecules are contained within (and hydrogenbonded to) the layered inorganic framework, the latter can act as a template, inducing different molecular packing than that achievable in a purely organic film. This control over packing has the potential for reducing the quenching interactions between the dye molecules, thereby increasing their overall luminescence quantum efficiency. Finally, the hybrid perovskite films exhibit a high thermal stability (120–200°C, depending on the inorganic framework) against grain growth, enabling more robust films. For comparison, glass transition temperatures of materials used in conventional OLEDs range from 60°C for common molecules such as N-N'-diphenyl-N-N' bis(3-methylphenyl)-[1-1'-biphenyl]-4-4'-diamine (TPD) to >150°C for starburst and related molecules [57].

The choice of oligothiophene dyes for this work was based on the ability to conveniently tune the electronic properties of the organic cation by tailoring the length of the oligothiophene moiety. Previous attempts to utilize thin, purely organic films of oligothiophene derivatives yielded less efficient OLEDs, with EL quantum yields ranging from  $10^{-9}$  to  $10^{-2}\%$  [58, 59]. This is due primarily to the inherently low fluorescence quantum yield of oligothiophenes caused by effective intersystem crossing [60, 61]. The efficiency of the preliminary hybrid perovskite devices ( $\sim$ 0.2 lm/W) is therefore quite promising, and higher values are expected with further fine tuning of the device structure, especially through

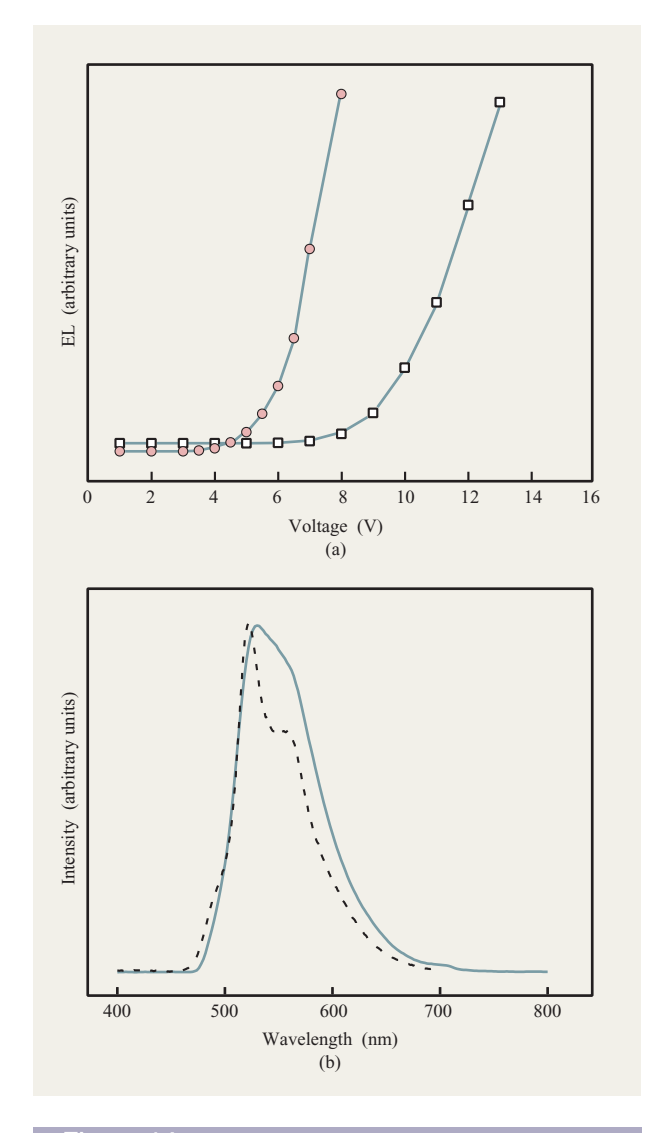
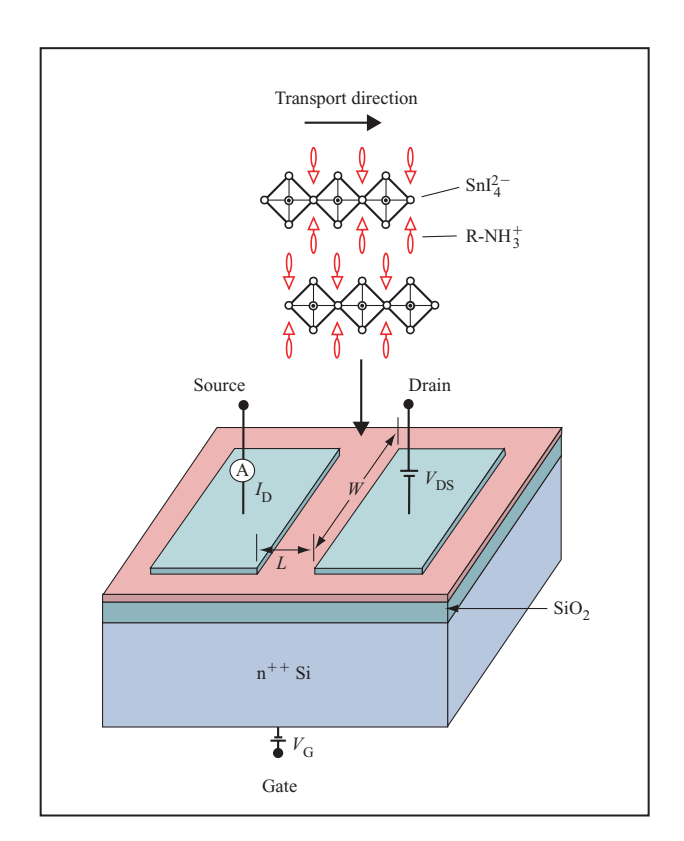


Figure 14

(a) Room-temperature electroluminescence–voltage (EL–V) characteristics of an OILED with a 3000-Å layer of (H<sub>2</sub>AEQT)PbCl<sub>4</sub> (filled circles), and one with a 1200-Å layer of (H<sub>2</sub>AEQT)CdCl<sub>4</sub> (open squares). (b) Room-temperature electroluminescence (solid curve) and photoluminescence (dashed curve, excited at 360 nm) spectra of an (H<sub>2</sub>AEQT)PbCl<sub>4</sub> film.

the incorporation of chromophores with fundamentally better fluorescence quantum yields. Appropriate modification of a wide range of structurally compatible dye molecules should provide a repertoire of candidate cations and also enable the realization of different emission colors (e.g., blue, red)—a requirement for full-color display applications. Other inorganic frameworks, currently under study, along with further understanding of the role of the inorganic component, should also help to improve device characteristics.





Schematic diagram of a TFT device structure employing a layered organic-inorganic perovskite as the semiconductor channel.

As an additional consideration for OILEDs, given the potentially high carrier mobilities and the tunable electronic structure achievable within the hybrid perovskite framework, these materials (even with optically inert organic cations) may be employed as carrier transport layers within LED device structures. For example,  $[C_6H_5(CH_3)CHNH_3]_2PbX_4$  (X = Cl, Br) perovskites have recently been demonstrated as hole transport layers (p-type semiconductors) in an OILED with a conventional organic emitter layer of poly(N-vinyl carbazole) (PVK) doped with the laser dye Coumarin 6 [62]. It was found that using lead(II) chloride inorganic perovskite sheets resulted in almost a tenfold improvement in efficiency compared to the use of lead(II) bromide layers. This improvement was attributed to the different band structures of the two perovskites and/or the better electron-blocking abilities of the lead chloride (higher-bandgap) perovskite.

In addition to their potential applications in OILED systems, semiconducting hybrid perovskites are also attractive as a new class of channel materials for thin-film field-effect transistors (FETs) [63]. The hybrid materials are interesting for this application because they can

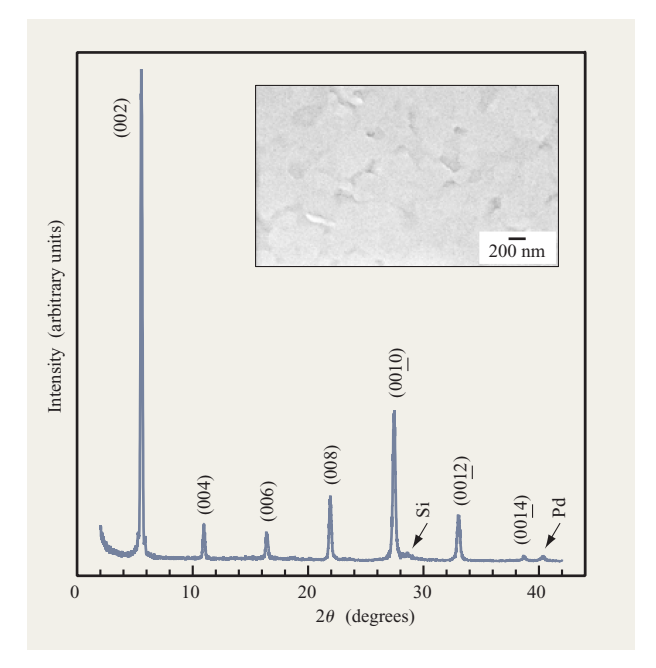


#### Figure 16

X-ray diffraction pattern for a completed TFT with  $(C_6H_5C_2H_4NH_3)_2SnI_4$  as the semiconducting channel and Pd source and drain electrodes. Inset is an SEM image of the hybrid perovskite film.

combine the higher carrier mobilities of ionic and covalently bonded inorganic semiconductors with the simple, low-cost and low-temperature thin-film techniques that make organic semiconductors exciting as alternative channel materials. Recently, we demonstrated the first organic-inorganic hybrid material as the semiconducting channel in a TFT, using the hybrid perovskite (C<sub>6</sub>H<sub>5</sub>C<sub>2</sub>H<sub>4</sub>NH<sub>3</sub>)<sub>2</sub>SnI<sub>4</sub> [63]. **Figure 15** depicts a typical organic-inorganic TFT device structure. Thin films of the hybrid perovskite are spin-coated from a methanol solution, in an inert atmosphere, onto thermally oxidized, degenerately n-doped silicon wafers. The SiO, layer acts as the gate insulator and is 400, 1500, or 5000 Å thick. The silicon wafer is used as the gate electrode, and highwork-function metals, such as Pd, Au, or Pt, are deposited by e-beam evaporation through silicon membrane masks and serve both as the source and drain electrodes and to define the channel dimensions. While the organicinorganic perovskite may be deposited either before or after metallization, depositing the source and drain electrodes before spin-coating eliminates exposing the hybrid perovskite films to potentially harmful metal deposition conditions (e.g., high temperatures).

Spin-coating single-layer (n = 1) tin(II) iodide perovskites with simple monoammonium organic cations results in oriented polycrystalline thin films having ~300-nm in-plane grain size. **Figure 16** shows the X-ray diffraction pattern and scanning electron micrograph (SEM) of a completed  $(C_6H_5C_2H_4NH_3)_2SnI_4$  TFT. The sharp X-ray diffraction pattern of only  $(0\ 0\ \ell)$  reflections and the smooth morphology seen in the SEM image are typical of spin-coated tin(II) iodide perovskites with simple monoammonium organic cations. The formation of extended inorganic sheets is also reflected in the prominent, sharp exciton peak in the optical absorption spectra at a wavelength  $(\lambda_{max} \approx 608\ nm)$  characteristic of the tin(II) iodide perovskite framework.

Field-modulated conductance in tin(II) iodide perovskites is observed for both simple aliphatic and aromatic organic cations, R-NH<sub>3</sub><sup>+</sup>. Each tin(II) iodidebased perovskite forms a p-channel transistor, consistent with previous Hall measurements [31, 39]. Figure 17 shows representative device characteristics for a TFT with the organic-inorganic perovskite (C<sub>6</sub>H<sub>5</sub>C<sub>2</sub>H<sub>4</sub>NH<sub>3</sub>)<sub>2</sub>SnI<sub>4</sub> as the channel layer and a 5000-Å-thick SiO<sub>2</sub> gate insulator layer. Application of a negative bias to the gate electrode  $(V_{\rm G} < 0)$  increases the number of majority holes in the semiconducting channel contributing to the drain current  $(I_{\rm D})$ . These devices show typical transistor-like behavior, as  $I_{\mathrm{D}}$  increases linearly at low source-drain voltage  $(V_{\mathrm{DS}})$ and then saturates as  $V_{\mathrm{DS}}$  increases and the holes in the channel are pinched off near the drain electrode. Application of a positive gate bias  $(V_{\rm G} > 0)$  depletes the holes in the channel, turning the device off.

The device characteristics of these organic-inorganic field-effect transistors (OIFETs) are modeled by the standard equations used for both inorganic and organic semiconducting channel materials. Figure 17(b) shows the dependence of  $I_{\rm D}$  and  $I_{\rm D}^{1/2}$  versus  $V_{\rm G}$ , at  $V_{\rm DS}=-100$  V. As determined from these curves, the field-effect mobility for the device is  $\mu = 0.61 \text{ cm}^2/\text{V-s}$ , and the  $I_{\text{ON}}/I_{\text{OFF}}$  ratio is  $\sim 10^6$ . These device characteristics are representative of (C<sub>6</sub>H<sub>5</sub>C<sub>2</sub>H<sub>4</sub>NH<sub>3</sub>)<sub>2</sub>SnI<sub>4</sub> and are comparable to the performance of amorphous silicon and the best organic semiconductors deposited in high vacuum. The reported  $I_{\rm ON}/I_{\rm OFF}$  ratio is achieved by crudely patterning the semiconducting perovskite, using a solvent-soaked cotton swab to remove material from around each device. By isolating devices, leakage current between source/drain electrodes and the back gate is effectively avoided. Unpatterned device structures show the same field-effect mobilities, but leakage current between gate and drain electrodes reduces the magnitude of current modulation. Similar device characteristics ( $\mu$  and  $I_{\rm ON}/I_{\rm OFF}$ ) are achieved at substantially lower applied voltages for devices fabricated using a thinner gate insulator.

Although  $(C_6H_5C_2H_4NH_3)_2SnI_4$  channels show the best device characteristics of the organic–inorganic TFTs prepared to date, tin(II) iodide perovskites with other organic molecules also show field-modulated conductance.

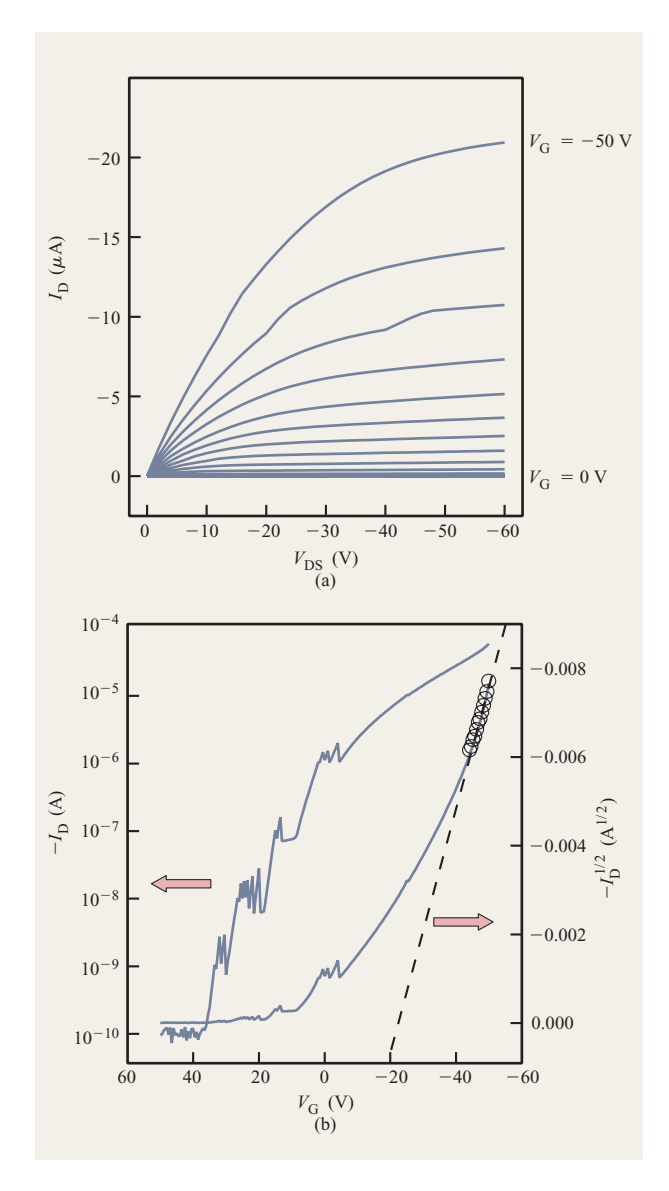


Figure 17

(a) Drain current  $I_{\rm D}$  versus source—drain voltage  $V_{\rm DS}$  as a function of gate voltage  $V_{\rm G}$  for a TFT with a spin-coated channel of  $({\rm C_6H_5C_2H_4NH_3)_2SnI_4}$ , a channel length  $L=28~\mu{\rm m}$ , and a channel width  $W=1000~\mu{\rm m}$ . The gate dielectric is 5000 Å of SiO $_2$ . (b) Plots of  $I_{\rm D}$  and  $I_{\rm D}^{1/2}$  versus  $V_{\rm G}$  at constant  $V_{\rm DS}=-100$  V, as used to calculate current modulation  $(I_{\rm on}/I_{\rm off})$  and field-effect mobility  $(\mu)$ .

Preliminary devices prepared with the alkylammonium tin iodides,  $(C_nH_{2n+1}NH_3)_2SnI_4$  (n=4 to 12), exhibit transistor-like behavior but have lower field-effect mobilities ( $\sim 10^{-3} - 10^{-2}$  cm²/V-s) compared to the phenethylammonium tin(II) iodide devices; they also do not completely turn off under positive gate bias. The inferior device performance may stem from differences in trap characteristics and/or in film and grain morphology

after spin-coating. Studies of the alkylammonium systems, along with other aromatic monoammonium and aliphatic diammonium cations, are continuing with the hope of further improving the mobility of the devices. One interesting opportunity involves the incorporation of extended aromatic cations that might achieve sufficient  $\pi$ - $\pi$  overlap to enable conduction in the organic layer of the structure, as well as in the inorganic layer. It might be possible, for example, to obtain effective hole transport in one of the layers and electron transport in the other. While tailoring the organic component in organic-

inorganic perovskites may be one means of controlling the mobility and conductivity of these materials, varying the perovskite dimensionality provides an alternate route. As mentioned above, increasing the number of inorganic tin(II) iodide sheets between each organic layer gives rise to a semiconductor-to-metal transition in bulk materials [31, 33]. The preparation of TFTs with n = 2 and n = 3 materials, in the family  $(C_4H_9NH_3)_2(CH_3NH_3)_{n-1}Sn_nI_{3n+1}$ , is currently under study. Preliminary results on  $(C_4H_0NH_3)_2(CH_3NH_3)Sn_2I_7$  (n = 2)channels show field-effect mobilities two orders of magnitude higher than that for the n = 1 material (C<sub>4</sub>H<sub>0</sub>NH<sub>3</sub>)<sub>2</sub>SnI<sub>4</sub>. Alternate inorganic semiconducting frameworks are also being explored to improve the stability of the OIFETs in air and to prepare both n- and p-type channel materials.

# **Conclusions**

Computer hardware relies intimately on inorganic and organic materials for the physical execution of computation processes and for displaying the results to the user. Crystalline silicon, for example, provides a highmobility framework (and a convenient and highly effective insulating oxide) for the construction of computer logic and memory components, as well as for display driver circuitry. New organic technologies, such as OLEDs and OFETs, are fast approaching commercial viability. Organic materials are particularly attractive because of the possibility of cheap, low-temperature processing and the range of interesting physical properties observed. While providing many important opportunities in their own right, organic and inorganic materials have limitations imposed by the chemistry and physics underlying each materials class. Consequently, combining the characteristics of organic and inorganic materials within a single molecularscale composite offers an important means of acquiring more functionality within the materials used to create new electronic and optical systems.

The organic-inorganic perovskites are one important class of crystalline hybrid materials that have recently received substantial attention. The inorganic component of the structure provides the potential for high electrical mobility, better thermal stability, magnetic and dielectric

transitions, and templating for the organic cations. The organic component can provide efficient fluorescence, simple processing, and the possibility of contributing to the electrical transport properties. By combining some of these characteristics within the hybrid perovskite framework, a number of important opportunities for organic–inorganic electronic devices have been proposed and, in some cases, demonstrated.

The highest-mobility spin-coatable (and processable at room temperature) FET channel has been fabricated, for example, using an organic-inorganic perovskite, with mobilities comparable to that of amorphous silicon. Higher mobility values can be expected as new, appropriately tailored organic-inorganic systems are examined. LEDs based on organic-inorganic perovskites have also been considered. By combining the efficient fluorescence of organic molecules with the templating and electronic band-structure tunability of metal halide sheets, relatively efficient OILEDs have been built with thick emission layers. Again, these are early results, and much better efficiencies are expected as more efficient dye molecules are incorporated into the perovskite framework.

Many other applications can be envisioned for the hybrid perovskites and similar organic–inorganic hybrids. For example, given the possibility of combining charge separation at an organic–inorganic interface with the high electrical mobility of an inorganic framework and the photosensitivity of an organic component, photoconductor and solar cell applications are worth considering [10]. In addition, the confinement of hyperpolarizable organic molecules within an inorganic framework provides substantial promise for nonlinear optical devices [64]. Other possibilities include novel materials for thermoelectric, dielectric, and magnetic applications. In each case, the exciting possibilities offered by organic–inorganic electronics are only beginning to be considered.

# **Acknowledgments**

The authors gratefully acknowledge the Defense Advance Research Projects Agency (DARPA) for partial support of this work under Contract No. DAAL01-96-C-0095.

#### References

- D. C. Edelstein, "Copper Chip Technology," Proc. SPIE— Int. Soc. Opt. Eng. (USA) 3506, 8 (1998).
- G. P. Crawford, "Liquid Crystal Displays," *IEEE Potentials* 17, 38 (1998).
- 3. J. Dresner, "Double Injection Electroluminescence in Anthracene," *RCA Rev.* **30**, 322 (1969).
- T. Wakimoto, H. Ochi, S. Kawami, H. Ohata, K. Nagayama, R. Murayama, Y. Okuda, H. Nakada, T. Tohma, T. Naito, and H. Abiko, "Dot-Matrix Display Using Organic Light-Emitting Diodes," *J. Soc. Info. Display* 5, 235 (1997).
- S. E. Shaheen, G. E. Jabbour, B. Kippelen,
  N. Peyghambarian, J. D. Anderson, S. R. Marder, N. R.

- Armstrong, E. Bellmann, and R. H. Grubbs, "Organic Light-Emitting Diode with 20 lm/W Efficiency Using a Triphenyldiamine Side-Group Polymer as the Hole Transport Layer," *Appl. Phys. Lett.* **74**, 3212 (1999).
- 6. (a) M. A. Baldo, S. Lamansky, P. E. Burrows, M. E. Thompson, and S. R. Forrest, "Very High-Efficiency Green Organic Light-Emitting Devices Based on Electrophosphorescence," *Appl. Phys. Lett.* **75**, 4 (1999); (b) T. Tsutsui, M.-J. Yang, M. Yahiro, K. Nakamura, T. Watanabe, T. Tsuji, Y. Fukuda, T. Wakimoto, and S. Miyaguchi, "High Quantum Efficiency in Organic Light-Emitting Devices with Iridium-Complex as a Triplet Emissive Center," *Jpn. J. Appl. Phys.* **38**, L1502 (1999).
- S. F. Nelson, Y. Y. Lin, D. J. Gundlach, and T. N. Jackson, "Temperature-Independent Transport in High-Mobility Pentacene Transistors," *Appl. Phys. Lett.* 72, 1854 (1998).
- C. D. Dimitrakopoulos, S. Purushothaman, J. Kymissis, A. Callegari, and J. M. Shaw, "Low-Voltage Organic Transistors on Plastic Comprising High-Dielectric Constant Gate Insulators," *Science* 283, 822 (1999).
- (a) G. Gustafsson, Y. Cao, G. M. Treacy, F. Klavetter, N. Colaneri, and A. J. Heeger, "Flexible Light-Emitting Diodes Made from Soluble Conducting Polymers," *Nature* 357, 477 (1992); (b) F. Garnier, R. Hajlaoui, A. Yassar, and P. Srivastava, "All-Polymer Field-Effect Transistor Realized by Printing Techniques," *Science* 265, 1684 (1994).
- (a) J. Takada, H. Awaji, M. Koshioka, A. Nakajima, and W. A. Nevin, "Organic-Inorganic Multilayers: A New Concept of Optoelectronic Material," *Appl. Phys. Lett.* 61, 2184 (1992); (b) J. Takada, "Organic-Inorganic Hetero Nanosystems as an Approach to Molecular Optoelectronics," *Jpn. J. Appl. Phys.* 34, 3864 (1995).
- 11. A. B. Seddon, "Sol-Gel Derived Organic-Inorganic Hybrid Materials for Photonic Applications," *IEEE Proc. Circuits Devices Syst.* **145**, 369 (1998).
- M. P. Andrews, "An Overview of Sol Gel Guest-Host Materials Chemistry for Optical Devices," Proc. SPIE— Int. Soc. Opt. Eng. (USA) 2997, 48 (1997).
- S. Motakef, J. M. Boulton, and D. R. Uhlmann, "Organic-Inorganic Optical Materials," Opt. Lett. 19, 1125 (1994).
- C. Roscher, R. Buestrich, P. Dannberg, O. Rösch, and M. Popall, "New Inorganic-Organic Hybrid Polymers for Integrated Optics," *Mater. Res. Soc. Symp. Proc.* 519, 239 (1998).
- M. Canva, B. Darracq, F. Chaput, K. Lahlil, F. Bentivegna, M. Brunel, M. Falloss, P. Georges, A. Brun, J.-P. Boilot, and Y. Lévy, "Functionalized Dye-Doped Hybrid Sol-Gel Materials: From Solid State Dye Laser to Nonlinear Applications and Organic Photorefractivity," Proc. SPIE—Int. Soc. Opt. Eng. (USA) 3469, 164 (1998).
- C. Sanchez and B. Lebeau, "Hybrid Organic–Inorganic Materials with Second-Order Optical Nonlinearities Synthesized via Sol–Gel Chemistry," *Pure Appl. Opt.* 5, 689 (1996).
- 17. S. Brasselet and J. Zyss, "New Routes in Molecular Nonlinear Optics: Sol-Gel Based Hybrid Structures and All Optical Orientation," *Proc. SPIE—Int. Soc. Opt. Eng.* (USA) **3469**, 154 (1998).
- H. K. Kim, S.-J. Kang, S.-K. Choi, Y.-H. Min, and C.-S. Yoon, "Highly Efficient Organic/Inorganic Hybrid Nonlinear Optic Materials via Sol-Gel Process: Synthesis, Optical Properties and Photobleaching for Channel Waveguides," *Chem. Mater.* 11, 779 (1999).
- T. Dantas de Morais, F. Chaput, K. Lahlil, and J.-P. Boilot, "Hybrid Organic-Inorganic Light-Emitting Diodes," Adv. Mater. 11, 107 (1999).
- For an example, see C. B. Murray, D. J. Norris, and M. G. Bawendi, "Synthesis and Characterization of Nearly

- Monodisperse CdE (E = S, Se, Te) Semiconductor Nanocrystallites," *J. Amer. Chem. Soc.* **115**, 8706 (1993).
- M. Brust, M. Walker, D. Bethell, D. J. Schiffrin, and R. Whyman, "Synthesis of Thiol-Derivatised Gold Nanoparticles in a Two-Phase Liquid-Liquid System," J. Chem. Soc., Chem. Commun., p. 801 (1994).
- C. B. Murray, C. R. Kagan, and M. G. Bawendi, "Self-Organization of CdSe Nanocrystallites into Three-Dimensional Quantum Dot Superlattices," *Science* 270, 1335 (1995).
- 23. C. R. Kagan, C. B. Murray, and M. G. Bawendi, "Long-Range Resonance Transfer of Electronic Excitations in Close Packed CdSe Quantum-Dot Solids," *Phys. Rev. B* **54**, 8633 (1996).
- C. P. Collier, R. J. Saykally, J. J. Shiang, S. E. Henrichs, and J. R. Heath, "Reversible Tuning of Silver Quantum Dot Monolayers Through the Metal-Insulator Transition," *Science* 277, 1978 (1997).
- V. Colvin, M. C. Schlamp, and A. P. Alivisatos, "Light-Emitting Diodes Made from Cadmium Selenide Nanocrystals and a Semiconducting Polymer," *Nature* 370, 354 (1994).
- B. O. Dabbousi, M. G. Bawendi, O. Onitsuka, and M. F. Rubner, "Electroluminescence from CdSe Quantum-Dot/Polymer Composites," *Appl. Phys. Lett.* 66, 1316 (1995).
- 27. M. C. Schlamp, X. Peng, and A. P. Alivisatos, "Improved Efficiencies in Light Emitting Diodes Made with CdSe(CdS) Core/Shell Type Nanocrystals and a Semiconducting Polymer," *J. Appl. Phys.* **82**, 5837 (1997).
- 28. D. B. Mitzi, "Synthesis, Structure, and Properties of Organic-Inorganic Perovskites and Related Materials," in *Progress in Inorganic Chemistry*, Vol. 48, John Wiley & Sons, Inc., New York, 1999, p. 1.
- D. B. Mitzi, "Organic-Inorganic Perovskites Containing Trivalent Metal Halide Layers: The Templating Influence of the Organic Cation Layer," *Inorg. Chem.* 39, 6107 (2000).
- 30. D. B. Mitzi, "(Phenethylammonium) $_2$ Cs $_{n-1}$ Sn $_n$ I $_{3n+1}$  (n=1 to 3): A New Class of Conducting Layered Organic/Inorganic Perovskites," *Bull. Amer. Phys. Soc.* **38**, 116 (1993).
- 31. D. B. Mitzi, C. A. Feild, W. T. A. Harrison, and A. M. Guloy, "Conducting Tin Halides with a Layered Organic-Based Perovskite Structure," *Nature* **369**, 467 (1994).
- J. Calabrese, N. L. Jones, R. L. Harlow, N. Herron, D. L. Thorn, and Y. Wang, "Preparation and Characterization of Layered Lead Halide Compounds," *J. Amer. Chem.* Soc. 113, 2328 (1991).
- 33. D. B. Mitzi, S. Wang, C. A. Feild, C. A. Chess, and A. M. Guloy, "Conducting Layered Organic-Inorganic Halides Containing (110)-Oriented Perovskite Sheets," *Science* **267**, 1473 (1995).
- 34. S. Wang, D. B. Mitzi, C. A. Feild, and A. Guloy, "Synthesis and Characterization of [NH<sub>2</sub>C(I)=NH<sub>2</sub>]<sub>3</sub>MI<sub>5</sub> (M = Sn, Pb): Stereochemical Activity in Divalent Tin and Lead Halides Containing Single (110) Perovskite Sheets," *J. Amer. Chem. Soc.* **117**, 5297 (1995).
- 35. G. C. Papavassiliou and I. B. Koutselas, "Structural, Optical and Related Properties of Some Natural Three-and Lower-Dimensional Semiconductor Systems," *Synth. Met.* **71**, 1713 (1995).
- 36. D. B. Mitzi, "Synthesis, Crystal Structure, and Optical and Thermal Properties of (C<sub>4</sub>H<sub>9</sub>NH<sub>3</sub>)<sub>2</sub>MI<sub>4</sub> (M = Ge, Sn, Pb)," *Chem. Mater.* **8**, 791 (1996).
- X. Hong, T. Ishihara, and A. V. Nurmikko, "Dielectric Confinement Effect on Excitons in PbI<sub>4</sub>-Based Layered Semiconductors," *Phys. Rev. B* 45, 6961 (1992).
- 38. T. Fujita, Y. Sato, T. Kuitani, and T. Ishihara, "Tunable Polariton Absorption of Distributed Feedback

- Microcavities at Room Temperature," *Phys. Rev. B* 57, 12428 (1998).
- D. B. Mitzi, C. A. Feild, Z. Schlesinger, and R. B. Laibowitz, "Transport, Optical, and Magnetic Properties of the Conducting Halide Perovskite CH<sub>3</sub>NH<sub>3</sub>SnI<sub>3</sub>," *J. Solid State Chem.* 114, 159 (1995).
- D. B. Mitzi, K. Chondroudis, and C. R. Kagan, "Design, Structure, and Optical Properties of Organic-Inorganic Perovskites Containing an Oligothiophene Chromophore," *Inorg. Chem.* 38, 6246 (1999).
- 41. M. Era, K. Maeda, and T. Tsutsui, "PbBr-Based Layered Perovskite Containing Chromophore-Linked Ammonium Molecule as an Organic Layer," *Chem. Lett.*, p. 1235 (1997).
- M. Braun, W. Tuffentsammer, H. Wachtel, and H. C. Wolf, "Tailoring of Energy Levels in Lead Chloride Based Layered Perovskites and Energy Transfer Between the Organic and Inorganic Planes," *Chem. Phys. Lett.* 303, 157 (1999).
- B. Servet, G. Horowitz, S. Ries, O. Lagorsse, P. Alnot, A. Yassar, F. Deloffre, P. Srivastava, R. Hajlaoui, P. Lang, and F. Garnier, "Polymorphism and Charge Transport in Vacuum-Evaporated Sexithiophene Films," *Chem. Mater.* 6, 1809 (1994).
- 44. F. Garnier, A. Yassar, R. Hajlaoui, G. Horowitz, F. Deloffre, B. Servet, S. Ries, and P. Alnot, "Molecular Engineering of Organic Semiconductors: Design of Self-Assembly Properties in Conjugated Thiophene Oligomers," J. Amer. Chem. Soc. 115, 8716 (1993).
- B. Tieke and G. Chapuis, "Solid State Polymerization of Butadienes in Layer Structures," *Mol. Cryst. Liq. Cryst.* 137, 101 (1986).
- P. Day and R. D. Ledsham, "Organic–Inorganic Molecular Composites as Possible Low-Dimensional Conductors: Photo-Polymerization of Organic Moieties Intercalated in Inorganic Layer Compounds," *Mol. Cryst. Liq. Cryst.* 86, 163 (1982).
- 47. H. Arend, W. Huber, F. H. Mischgofsky, and G. K. Richter-van Leeuwen, "Layered Perovskites of the (C<sub>n</sub>H<sub>2n+1</sub>NH<sub>3</sub>)<sub>2</sub>MX<sub>4</sub> and NH<sub>3</sub>(CH<sub>2</sub>)<sub>m</sub>NH<sub>3</sub>MX<sub>4</sub> Families with M = Cd, Cu, Fe, Mn, or Pd and X = Cl or Br: Importance, Solubilities and Simple Growth Techniques," *J. Cryst. Growth* 43, 213 (1978).
- 48. M. Era, T. Hattori, T. Taira, and T. Tsutsui, "Self-Organized Growth of PbI-Based Layered Perovskite Quantum Well by Dual-Source Vapor Deposition" *Chem. Mater.* **9,** 8 (1997).
- D. B. Mitzi, M. T. Prikas, and K. Chondroudis, "Thin Film Deposition of Organic-Inorganic Hybrid Materials Using a Single Source Thermal Ablation Technique," Chem. Mater. 11, 542 (1999).
- 50. K. Chondroudis and D. B. Mitzi, "Effect of Thermal Annealing on the Optical and Morphological Properties of (AETH)PbX<sub>4</sub> (X = Br, I) Perovskite Films Prepared Using Single Source Thermal Ablation," *Chem. Mater.* 12, 169 (2000).
- K. Liang, D. B. Mitzi, and M. T. Prikas, "Synthesis and Characterization of Organic-Inorganic Perovskite Thin Films Prepared Using a Versatile Two-Step Dipping Technique," *Chem. Mater.* 10, 403 (1998).
- X. Hong, T. Ishihara, and A. V. Nurmikko, "Photoconductivity and Electroluminescence in Lead Iodide Based Natural Quantum Well Structures," Solid State Commun. 84, 657 (1992).
- M. Era, S. Morimoto, T. Tsutsui, and S. Saito,
  "Organic-Inorganic Heterostructure Electroluminescent Device Using a Layered Perovskite Semiconductor (C<sub>6</sub>H<sub>5</sub>C<sub>2</sub>H<sub>4</sub>NH<sub>3</sub>)<sub>2</sub>PbI<sub>4</sub>," Appl. Phys. Lett. 65, 676 (1994).
- 54. T. Hattori, T. Taira, M. Era, T. Tsutsui, and S. Saito, "Highly Efficient Electroluminescence from a Heterostructure Device Combined with Emissive Layered-

- Perovskite and an Electron-Transporting Organic Compound," Chem. Phys. Lett. 254, 103 (1996).
- K. Chondroudis and D. B. Mitzi, "Electroluminescence from an Organic-Inorganic Perovskite Incorporating a Quaterthiophene Dye Within Lead Halide Perovskite Layers," Chem. Mater. 11, 3028 (1999).
- W. Rie, H. Riel, P. F. Seidler, and H. Vestweber, "Organic-Inorganic Multilayer Structures: A Novel Route to Highly Efficient Organic Light-Emitting Diodes," Synth. Met. 99, 213 (1999).
- 57. Y. Kuwabara, H. Ógawa, H. Inada, N. Noma, and Y. Shirota, "Thermally Stable Multilayered Organic Electroluminescence Devices Using Novel Starburst Molecules, 4,4',4"-Tri(N-carbazolyl)triphenylamine (TCTA) and 4,4',4"-Tris(3-methylphenyl-phenylamino)triphenylamine (m-MTDATA), as Hole-Transport Materials," Adv. Mater. 6, 677 (1994).
- K. Uchiyama, H. Akimichi, S. Hotta, H. Noge, and H. Sakaki, "Electroluminescence from Thin Film of a Semiconducting Oligothiophene Deposited in Ultrahigh Vacuum," Synth. Met. 63, 57 (1994).
- 59. G. Horowitz, P. Delannoy, H. Bouchriha, F. Deloffre, J.-L. Fave, F. Garnier, R. Hajlaoui, M. Heyman, F. Kouki, P. Valat, V. Wintgens, and A. Yassar, "Two-Layer Light-Emitting Diodes Based on Sexithiophene and Derivatives," *Adv. Mater.* 6, 752 (1994).
- S. Rentsch, J. P. Yang, W. Paa, E. Birckner, J. Schiedt, and R. Weinkauf, "Size Dependence of Triplet and Singlet States of α-Oligothiophenes," *Phys. Chem. Chem. Phys.* 1, 1707 (1999).
- D. Grebner, M. Helbig, and S. Rentsch, "Size-Dependent Properties of Oligothiophenes by Picosecond Time-Resolved Spectroscopy," J. Phys. Chem. 99, 16991 (1995).
- 62. T. Gebauer and G. Schmid, "Inorganic-Organic Hybrid Structured LED's," Z. Anorg. Allg. Chem. 625, 1124 (1999).
- 63. C. R. Kagan, D. B. Mitzi, and C. Dimitrakopoulos, "Organic-Inorganic Hybrid Materials as Semiconducting Channels in Thin-Film Field-Effect Transistors," *Science* **286**, 945 (1999).
- 64. J. Pecaut, Y. Le Fur, and R. Masse, "Crystal Engineering and Structural Investigations of the 2-Amino-5-Nitropyridinium Salts  $C_5H_6N_3O_2^+ \cdot HSO_4^-$  and  $C_5H_6N_3O_2^+ \cdot H_2ASO_4^-$ ," Acta Crystallogr. B 49, 535 (1993).

Received October 2, 1999; accepted for publication August 11, 2000

David B. Mitzi IBM Research Division. Thomas J. Watson Research Center, P.O. Box 218, Yorktown Heights, New York 10598 (dmitzi@us.ibm.com). Dr. Mitzi is a Research Staff Member in the Physical Sciences Department at the Thomas J. Watson Research Center. He received a B.S.E. degree in electrical engineering (with a certificate in engineeringphysics) from Princeton University in 1985 and a Ph.D. degree in applied physics from Stanford University in 1990. In 1990, he joined the IBM Research Division and has since been examining the solid-state chemistry and thinfilm deposition and device opportunities for a variety of materials with interesting and potentially useful electronic and/or optical properties. Since 1993, his focus has been on a family of organic-inorganic hybrids, with the goal of creating useful materials for LED and FET applications. Dr. Mitzi is a member of the American Chemical Society, the American Physical Society, and the Materials Research Society. He has authored or coauthored more than a hundred papers and holds several patents.

Konstantinos Chondroudis Symvx Technologies Inc., Santa Clara, California (kchondroudis@symyx.com). Dr. Chondroudis is currently a Staff Scientist at Symyx Technologies Inc. in Santa Clara, California, where his research efforts are directed toward the development of combinatorial methods for synthesizing and screening solid-state materials. From 1997 to 1999, he worked as a postdoctoral scientist at the IBM Thomas J. Watson Research Center in Yorktown Heights, New York, researching the applications of organic-inorganic hybrid materials in organic light-emitting diodes (OLEDs) and other electronic devices. Dr. Chondroudis received his B.S. degree in chemistry from Aristotle University in Thessaloniki, Greece, in 1993 and his Ph.D. degree in inorganic chemistry from Michigan State University in 1997. He is a member of the American Chemical Society and the Materials Research Society.

Cherie R. Kagan IBM Research Division, Thomas J. Watson Research Center, P.O. Box 218, Yorktown Heights, New York 10598 (cheriek@us.ibm.com). Dr. Kagan is a Research Staff Member in the Physical Sciences Department at the IBM Thomas J. Watson Research Center. She received a B.S.E. degree in materials science and engineering and a B.A. degree in mathematics, both from the University of Pennsylvania, in 1991. In 1996, she received her Ph.D. degree in electronic materials from MIT. Her thesis work focused on the selfassembly of close-packed solids of semiconductor nanocrystals and the unique electronic and optical properties that arise from cooperative interactions between neighboring nanocrystals. In 1996, Dr. Kagan went as a Postdoctoral Fellow to Bell Laboratories, where she built a scanning confocal Raman microscope to study the formation of holograms in multicomponent photopolymers. In 1998 she joined IBM, where she has been investigating the optical and electrical properties of organic-inorganic hybrid materials and the application and patterning of organic-inorganic hybrids and soluble organic semiconductors in thin-film field-effect transistors.